UCRL-JC-124536 Rev 1
PREPRINT

Laser Intensity Modulation by Nonabsorbing Defects

M. D. Feit
A. M. Rubenchik

This paper was prepared for submittal to the
2nd Annual International Conference on
Solid-State Lasers for Application to ICF
Paris, France
October 22-25, 1996

January 24, 1997

Lawrence Livermore National Laboratory

DISCLAIMER

Laser Intensity Modulation by Nonabsorbing Defects

M.D. Feit, A.M. Rubenchik
Lawrence Livermore National Laboratory
7000 East Avenue, mail stop L-439
Livermore, CA 94550

Abstract

Nonabsorbing bulk defects can initiate laser damage in transparent materials. Defects such as voids, microcracks and localized stress concentrations can serve as positive or negative lenses for the incident laser light. The resulting interference pattern between refracted and diffracted light can result in intensity increases on the order of a factor of 2 some distance away from a typical negative microlens, and even larger for a positive microlens. Thus, the initial damage site can be physically removed from the defect which initiates damage. The parameter that determines the strength of such lensing is $(Ka)^2\,\Delta\varepsilon$ where the wavenumber K is $2\pi/\lambda$, 2a is the linear size of the defect and $\Delta\varepsilon$ is the difference in dielectric coefficient between matrix and scatterer. Thus, even a small change in refractive index results in a significant effect for a defect large compared to a wavelength. Geometry is also important. Three dimensional (eg. voids) as well as linear and planar (eg. cracks) microlenses can all have strong effects.

The present paper evaluates the intensification due to spherical voids and high refractive index inclusions. We wish to particularly draw attention to the very large intensification that can occur at inclusions.

Introduction

The danger posed by absorbing defects in a transparent substrate has long been recognized and understood [1]. Such defects absorb energy, heat and expand, thereby thermally and mechanically stressing the surrounding material. It is also known that pure diffractive (eg. clipping at pinhole) effects in high power laser systems can lead to laser induced damage by causing intensity modulations that seed nonlinear self-focusing [2,3]. In this case, nonlinear refraction raises the intensity level above the damage threshold.

We wish to point out that for high power laser systems, intensity modulations due to purely transparent defects may be capable of inducing damage without invoking any nonlinear effects. Both negative (eg. voids) and positive (eg. high refractive index inclusion) defects scatter light strongly resulting in large intensity modulation. High refractive index inclusions are especially dangerous since they act like efficient focusing lenses.

Formulation

The situation of interest here is in the borderline area of wave optics and geometric optics. Very small defects (size comparable with a wavelength) with refractive index not very much different from that of the surrounding material can be treated by perturbative methods (Born approximation, WKB, etc.) or treated by paraxial wave propagation. In the present case, we are interested in defects many wavelengths in size with very large differences in refractive index (eg. -0.5 for a void up to +0.6 for a pure zirconia inclusion). This situation cannot be treated by paraxial optics since it involves strong reflections including total internal reflections inside an inclusion.

The vector theory of electromagnetic scattering was worked out by Mie; it is described in the classic book of Van de Hulst[4]. To be definite here, we choose to model spherical defects for which the solution can be calculated in a convenient form. In the case of larger (compared with wavelength) spheres, it is adequate to use the scalar approximation familiar from spherical scattering in the Schroedinger equation[5] .

That is, we wish to solve the scalar wave equation

$$\nabla^2 E + k_0^2\, \eta(\vec{r})^2 E = 0 \qquad (1)$$

where k_0 is the free space wavenumber $2\pi/\lambda$, and $\eta(r)$ is the spatially dependent refractive index. The refractive index is assumed to have the value η_1 inside a sphere of radius a, and the value η_2 outside this sphere. For convenience, we define the material wavenumbers $k_{1,2} = k_0\, \eta_{1,2}$. Then, the solution can be written as a superposition of spherical waves of the form

$$E = \sum_{l=0}^{\infty} (2l + 1)\, i^l \exp(i\delta_l) \left(j_l(k_2 r) \cos(\delta_l) - n_l(k_2 r) \sin(\delta_l)\right) P_l(\cos\theta) \qquad (2)$$

Here j_l and n_l are spherical Bessel functions and P_l is a Legendre polynomial. The effect of the scatterer centered at r=0 is given by the phase shifts δ_l which vanish identically for no scatterer. The phase shifts are determined from a transcendental eigenvalue equation

$$\tan(\delta_l) = \frac{k_2\, j_l'(k_2 a) - \gamma_l j_l(k_2 a)}{k_2\, n_l'(k_2 a) - \gamma_l n_l(k_2 a)} \qquad (3)$$

where

$$\gamma_l = \frac{k_1\, j_l'(k_1 a)}{j_l(k_1 a)} \qquad (4)$$

and the primes denote differentiation with respect to argument.

Although there are an infinite number of terms in the summation in Eq.(2) , the number of partial wave phase shifts δ_l appreciably affected by the scattering is proportional to the size of the scatterer, ie. roughly equal to ka . This effect is shown in Fig. (1) where phase shifts δ_l corresponding to three sizes of void in glass are compared. Larger defects perturb larger numbers of partial waves. This is why it is computationally difficult to treat very large defects.

It is believed that very small (less than say 25 μm) voids and inclusions are not likely to occur in laser glass because of their tendency to dissolve during fabrication. The calculations reported here are for small defects since these are much easier to calculate. The intensifications important for damage initiation only become larger and persist over longer distances for larger defects. On the other hand, spherical defects probably exhibit the largest magnitude effect, especially for large refractive index inclusions. Actual defects need not be spherical, of course. Our results serve to point out the large intensifications which can result from transparent defects.

Voids

The distribution of intensity around a typical small spherical void (refractive index unity) in fused silica is shown in Fig. 2. A plane wave of intensity unity is incident from above. Because the refractive index in the void is lower than that of fused silica, the void acts like a thick diverging lens. From a geometric optics picture, light rays are bent strong away from the axis leaving a "shadow" region behind the void. It is the intensity modulations on the edge of this shadow that concern us here. Intensity maxima of twice the incident intensity occur in the vicinity of the void. Further away, these maxima tend to die out as is shown in Fig. 3 which exhibits transverse intensity modulations at different distances from the void. These modulations die out more slowly for larger voids (over a distance comparable with the Raleigh range Ka^2).

Inclusions

Defects with larger refractive index than the surrounding material are more dangerous since they act as concentrating lenses. These are not simple lenses, of course, because they are "thick", ie there is a large variation in optical path length over the incoming beam. Consider a spherical inclusion of radius a. The phase variation experienced by straight ahead rays passing through the sphere is given by

$$\Delta\phi = 2\,K\,a\,(\Delta n/n)(1 - (x/a)^2)^{1/2} \qquad (5)$$

at transverse position $x<a$. Here $\Delta n/n$ is the relative change in refractive index. Expanding the square root yields a simple estimate for the effective focal length as $a/(2\,\Delta n/n)$. This estimate is reasonably borne out by the waveoptical calculations, especially in that the focal length is proportional to the size of the sphere. The full calculation has to be carried out, however, to determine the intensity at the (aberrated) focus.

The intensification factor can be large, even when the change in refractive index is small. Fig. 4 plots the axial intensity (in units of the input intensity) downstream from a 4 μm sphere of index 1.51 in a silica (n=1.5) substrate. The inclusion is centered at z=0. The maximum intensity outside the defect is about 1.5 . A modest increase in refractive index of the inclusion to 1.6 increases the maximum intensity to 10 times the initial intensity (Fig. 5).

An example of truly impressive intensification is seen for zirconia (n=2.1) inclusions. Fig. 6 shows the axial intensity downstream of a 12 μm inclusion. The peak intensity is about 1000 times the plane wave intensity at a distance of about 9 μm from the inclusion center. The transverse intensity variation at the peak (Fig. 7) exhibits a typical Airy pattern-like distribution in the central region. Outside of this is a low intensity region from which light has been totally internally reflected by the inclusion surface. This general picture can be seen from simple ray tracing (Fig. 8) although only the wave treatment allows one to determine the degree of intensification.

Conclusions

Spherical voids and inclusions in glass can lead to significant intensity modulation of an otherwise flat input beam. High refractive index inclusions are especially dangerous since they act as focusing lenses and can lead to very high axial intensities. The cases calculated here are for inclusions smaller than that which probably occur. Since the intensification scales with the defect size, larger inclusions will yield higher intensification.

Of course, "real" defects might not be perfectly spherical so the above is a worse case scenario. Also, if there is mixing of materials during glass fabrication, one might end up with a region of refractive index intermediate between 1.5 and that of the impurity . Also, it should be noted that strong intensification can occur inside the inclusion itself. This interior intensification may damage the inclusion and lessen the exterior focusing effect. Very small (pure) inclusions should not occur because of the glass fabrication process. The worrisome range in which presently undetected inclusions might occur is approximately 20-80 μm in size .

Despite all these caveats, the large size of the effect calculated here implies that any such inclusions are unacceptable from the viewpoint of laser damage.

This work was performed under the auspices of the U.S. DOE by LLNL under contract no. W-7405-Eng-48.

references

[1] See, e.g., Modeling laser damage caused by platinum inclusions in laser glass, J.H. Pitts, Laser Induced Damage in Optical Materials:1985, Boulder Damage Symposium, NBS Special Publication 746 (1986)

[2] Study of self-focusing damage in a high power Nd:glass amplifier, J.A. Fleck, Jr. and C. Layne, Appl. Phys. Lett. **22**, 467-9 (1973)

[3] Diffraction and self-focusing during amplification of high power light pulses I. Development of diffraction and self focusing in an amplifier, N.B. Baranova, N.E. Bykovskii, B. Ya. Zel'dovich and Yu. V. Senatskii, Kvant. Electr. **1**, 2435-49 (1974), translated in Sov. J. Quant. Electr. **4**, 1354- 61(1975)

[4] *Light Scattering by Small Particles*, H.C. Van de Hulst, (John Wiley, New York, 1957)

[5] *Quantum Mechanics*, 3rd Edition, L.I. Schiff, (McGraw-Hill Book Company, New York, 1968)

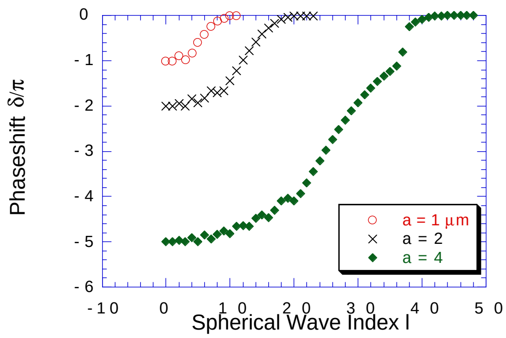

Fig. 1 : Partial wave phase shifts of Eq(2) for void in glass. The number of significant phase shifts is proportional to the size of the void.

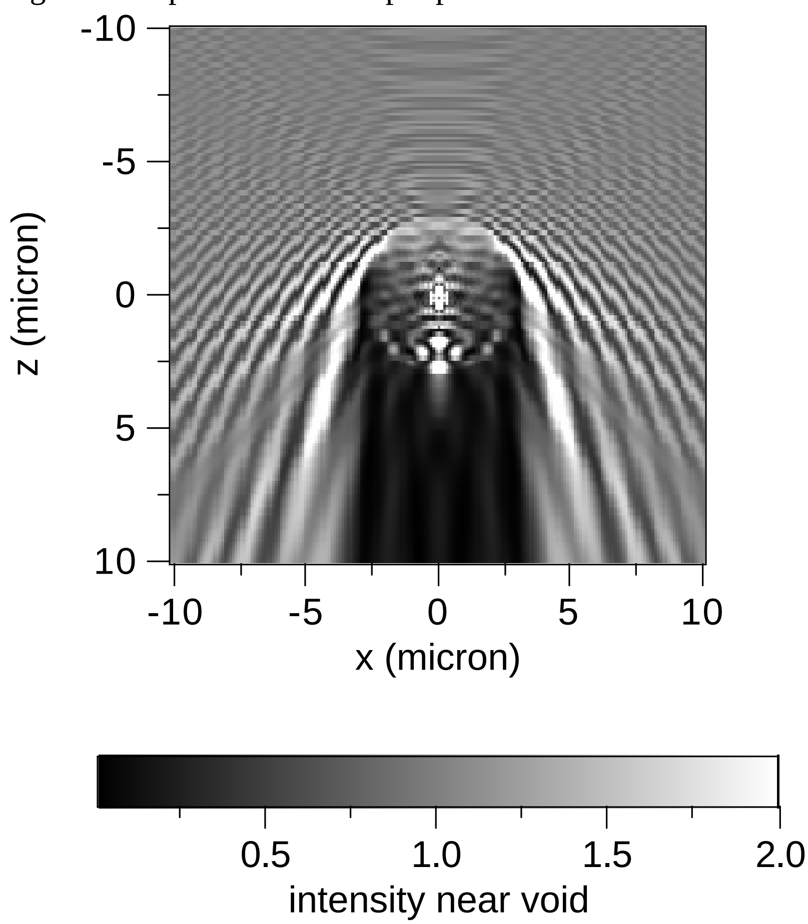

Fig. 2 : Distribution of intensity in vicinity of small spherical void in glass. Light incident from top. Note shadow region behind void and intensity modulations.

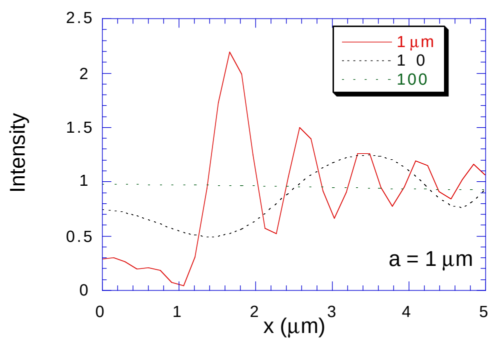

Fig. 3: Transverse intensity modulations near 2 µm void. Modulation of 100% just outside void; nearly gone at distance of 100 µm.

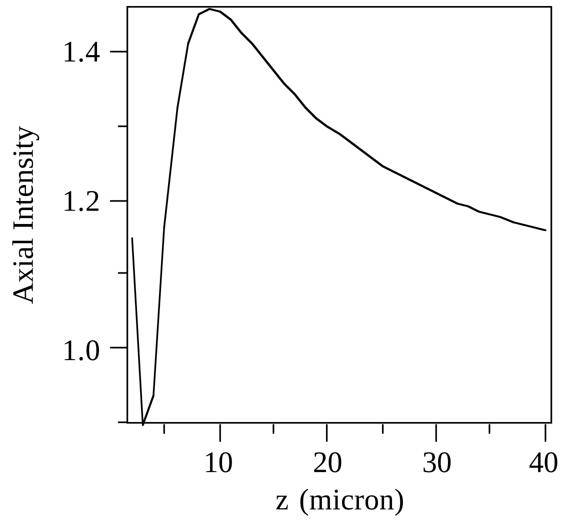

Fig. 4: Axial intensity near 4 µm inclusion with refractive index 1.51 . Intensification (1.5 in this case) depends on Δn and size of inclusion.

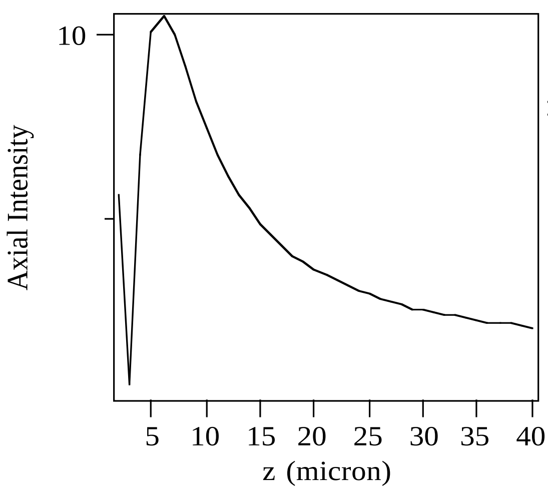

Fig. 5: Axial intensity near 4 µm inclusion with refractive index 1.6 .

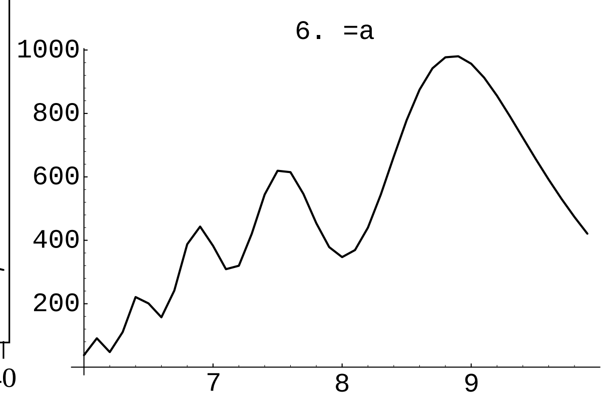

Fig. 6: Axial intensity variation downstream of a 6 µm radius zirconia inclusion (n=2.1)

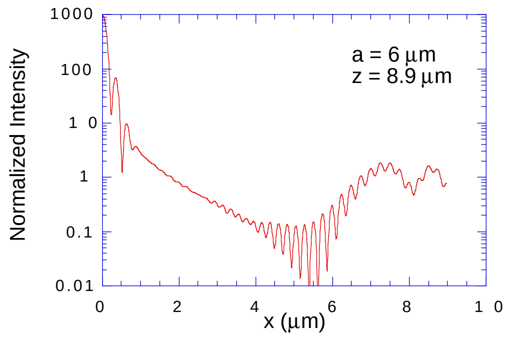

Fig. 7: Transverse intensity variation downstream of 6 µm radius zirconia inclusion.

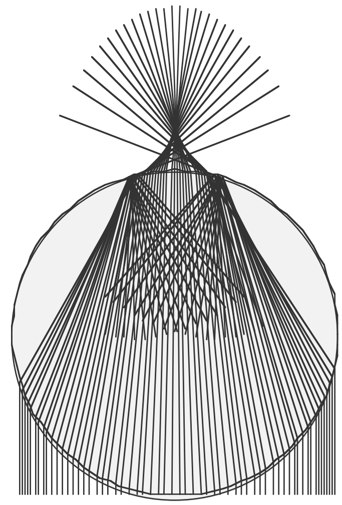

Fig. 8: Ray tracing through zirconia sphere in silica. Inner rays come to focus. Outer rays internally reflect.

Technical Information Department • **Lawrence Livermore National Laboratory**
University of California • Livermore, California 94551